Available online www.jsaer.com

***Journal of Scientific and Engineering Research*, 2019, 6(12):235-252**

Research Article

ISSN: 2394-2630
CODEN(USA): JSERBR

Onset of Rayleigh-Benard convection in CO_2 Sequestration in the Anisotropic Porous Medium within Eastern Niger Delta Region

T.I. Okeke, C. Israel-Cookey, E.D. Uko, M.A. Alabraba

Department of Physics, Rivers State University, Port Harcourt, Nigeria

Abstract The stability of convection in a porous medium (specifically the anisotropic porous medium), where the concentration of solute is assumed to decay via first-order chemical reaction within Eastern Niger-Delta region, Nigeria, is studied. A simplified model is envisaged for the interactive relationship between carbon dioxide and ambient brine in deep underground aquifers; the instability which is a favorable process for CO_2 sequestration considering the fact that it accelerates dissolution and mixing of CO_2 hence, reducing the time needed to safely store CO_2 in the aquifer. The time scale for the onset of convection as indicated by diverse linear stability analyses of the short-term base state may be long (for years) but virtually will without a doubt be notably shortened by mixing during injection of supercritical CO_2.

The key purpose of this paper is to explore the role porous media anisotropy plays in the onset of convective instability of sequestered CO_2 in the underground aquifer. It is shown that for changes of permeability, varying the ratio of horizontal solutal and thermal diffusivities to vertical solutal and thermal diffusivities at values less than 1 ($\xi < 1$) in the anisotropic porous medium presents a more suitable medium for convective instability of sequestered CO_2. Thus, at $\xi < 1$, the anisotropic porous medium presents a suitable medium for convective instability even at low permeability and in turn reduces the time needed to safely store CO_2 in the deep saline aquifer. It is also observed that the ratio of thermal diffusivity to mass diffusivity (the Lewis Number), lower values of the Damköhler number ($Da = 0.0001, 0.001, 0.01$) and the presence of the Solute Rayleigh number, delays the onset of instability of sequestered CO_2 in the system in the anisotropic porous medium. However, interestingly, at a high solute reaction rate to diffusion rate (increasing Damköhler number from $Da = 0.1$ to $Da = 0.2$), a change in permeability of the porous medium does have a pronounced effect on instability in the anisotropic porous medium only at $\xi < 1$.It is now known that areas within the Eastern Niger Delta region will be suitable for CO_2 sequestration especially areas dominated by the anisotropic porous medium, were a short-term amount of carbon dioxide dissolves speedily because the onset of instability here is rapid.

Keywords CO_2 sequestration, Rayleigh-Benard convection, First-order chemical reaction, Temperature gradient, Stability analysis, Anisotropic Porous Medium

Variables

CO_2	Carbon dioxide
κ_T	Thermal Conductivity of the Saturated Porous Medium
α_T	Effective Thermal Diffusivity through the Fluid in the Porous Medium
	Dimensionless Porosity
Le	Lewis Number, the Ratio of Thermal Diffusivity through the Fluid to Mass or Solute Diffusivity
P	Pressure [$kgm^{-1}s^{-2}$]
U	Velocity Vector (u, v, w) [ms^{-1}]
Ra	Darcy – Rayleigh Number

Rs	Solute Rayleigh Number
C	Solute Concentration
T	Temperature [K]
$k_r a$	The Reaction Rate Constant Based on the Solid Surface Area per Unit Volume of the Porous Medium
K	Effective Variable Permeability
g	Gravitational Acceleration [ms^{-2}]
K_0	Reference permeability
β_T	Thermal Expansion Coefficient
β_C	Solute Expansion Coefficient
κ_C	Solute Diffusivity
Da	Damköhler Number, the Ratio of Solute Reaction to Diffusion Rates
ϕ	Porosity of the Matrix
k	Direction of Vector Field
σ	Growth Rate
ξ	Anisotropy Parameter
κ_h	Horizontal Solute and Thermal Diffusivity
κ_z	Vertical Solute and Thermal Diffusivity
μ	Fluid Viscosity [Nsm^{-2}]
ρ	Density [kgm^{-3}]
ρ_0	Reference Density
ΔT	Temperature Difference between the Walls
ΔC	Solute Difference between the Walls
a_x	Wave Number in the x – direction
a_y	Wave Number in the y – direction
γ	Ratio of Heat Capacities
x, y, z	Space Coordinates
$(\rho C_P)_m$	Volumetric Heat Capacity of the Saturated Medium
$(\rho C_P)_f$	Volumetric Heat Capacity of the Fluid

Superscripts

$*$	Dimensioned Quantity
s	Stationary State

Subscripts

b	Basic State
f	Fluid
m	Medium (Porous Medium)

1. Introduction

Emission of Carbon dioxide takes place in two ways. Emission from fixed sources (Industry, Heating and Power generation) and emission from mobile sources (Cars and Trucks). The fixed-source emits about two-third of the total CO_2 emission, while the mobile-sources emit the remainder. About sixty percent of fixed-source emissions are large scale and occurs at specific locations and thus are amenable to CO_2 control strategies, such as CO_2 capture and storage, albeit at an economic cost. Globally, an estimate of about 34% increase in CO_2 emission is envisaged between 2012 – 2040 from 30 Billion metric tonnes to over 40 Billion metric tonnes of CO_2. Nigeria is one amongst five countries known to have emitted nearly 0.5 Gigatonnes of CO_2 presently. Alternative renewable source of energy could be used in place of fossil fuels as an effective way of reducing carbon dioxide content stored in the atmosphere. This alone will call for a long-term intensive research and development to

create new technological options. As these long-term options are being processed, an immediate and accessible plan of action to reduce the accumulation of CO_2 in the atmosphere is its storage in underground brine-filled aquifers [1].

Convection, which gives rise to instability in fluids occurs as a result of buoyancy effect when heat energy is transported by the motion of particles in a fluid, in which the heating of the fluid is from below making the fluid at the bottom lighter than the fluid at the top. A fluid system could be gravitationally unstable as a result of CO_2 injection into a geologically stable formation (deep saline aquifer). The less dense CO_2 rises towards the top of the formation and gets trapped under an impermeable cap rock as a separate free phase. As natural/density-driven convection sets in, the CO_2 dissolves gradually into the brine forming the CO_2-saturated brine having a higher density than pure brine at the top of the formation [2-3]. This thick carbon-rich brine layer is formed on top an impermeable carbon-free and lighter brine layer. Thus, a two phase CO_2 and brine interface is formed at the top of the aquifer.

Convective instability in a porous media was first addressed by Horton & Rogers [4] and independently by Lapwood [5]. They considered a saturated porous layer of infinite horizontal extent, such that the bottom temperature is hotter than the top temperature. In their independent research, they claimed that there were naturally occurring geothermal gradients in the subsurface which led to an assumption that temperature increases linearly with depth. They also examined buoyancy-driven convection in a porous medium using stability analysis now referred to as Rayleigh-Benard convection. In the Rayleigh-Benard convection, Rayleigh showed that the system remains stable provided the thermal Rayleigh number **R**, remains less than the critical Rayleigh value $(\mathbf{R_C = 4\pi^2})$. But when $\mathbf{R \geq R_C}$ the system becomes unstable and thermal convection sets in, in the form of a convection pattern where fluid circulation transports heated mass upwards and colder mass downwards. Getling [6] in addition also stressed that the Rayleigh number and Prandtl number are the basic dimensionless parameters controlling the convection regime. In concurrence with the Rayleigh-Benard convection, Getling showed using neutral curves convectively unstable layers where $\mathbf{R>R_C}$ and stable layers at $\mathbf{R<R_C}$while convection sets first at $\mathbf{R= R_C}$**.** Adopting the methods developed for Rayleigh-Benard convection, Caltagirone [7] studied thermally driven convection by also considering the fact that temperature increases linearly with depth which is appropriate for gradual heating systems. In addition to this, he analyzed the effect of transient base temperature field and their boundary layer characteristics in a porous medium. Ennis-King et al. [8] applied the methods adopted by Caltagirone's analysis to CO_2 sequestration problem into anisotropic porous media. Haddad [9] and Vadasz [10] both considered thermal convection in a rotating saturated porous medium layer. In contrast with the article by Vadasz, Haddad considered the anisotropic porous medium viewing a scenario wherein the permeability in the vertical direction is distinct from that in the horizontal plane. Xu et al. [11]; Rapaka et al. [12] and Hassanzadeh et al. [13] contributed to the investigation in connection with the CO_2 storage in saline aquifers. In their independent research, they solved the stability equation in a layer of uniform thickness. Riaz et al. [14]; Selim and Rees [15] and Wessel-Berg [16] analyzed the onset of convection in a porous media under the time dependent temperature or concentration field in the semi-infinite domain with claims that the analysis will yield accurate stability criteria when the basic fields have the boundary-layer characteristics. De Paoli et al. [17] examined the role of anisotropic permeability in the distribution of solutal concentration in fluid saturated porous medium. They came to a conclusion that in the anisotropic sedimentary rocks, the short term amount of carbon dioxide that can be dissolved is much greater than in isotropic rocks. Alex et al. [18]; Malashetty and Swamy [19]; Vanishree et al. [20] and Kumar et al. [21] all studied the onset of convection/thermal instabilities in a rotating anisotropic porous medium, adopting either or both the nonlinear stability theory or/and the linear instability theory in their various research. In addition, Malashetty and Biradar [22] investigated the effect of reaction rate, Lewis number, mechanical and thermal anisotropy parameters, normalized porosity and solute Rayleigh number on the stability of the system of a horizontal anisotropic porous layer.

Effect of geochemical reaction on the onset of buoyancy-driven convection in CO_2 sequestration process has been reported in the literature by Ghesmat et al. [23]. They analyzed the effect of second-order geochemical reaction on the buoyancy-driven convection in a porous medium. They suggested that the effects of reaction order are negligible when the Damköhler number and time are small but when the Damköhler number and time

is large enough, the rates of reaction and concentration changes for a first order reaction faster than for a second order reaction. Andres and Cardoso [24, 25] analyzed the impact of chemical reaction on the onset of buoyancy-driven convection through the numerical simulation. In their work, they considered a first order reaction which occurs between dissolved solute and a chemical specie in the solid matrix. From their numerical simulations, they observed that convective motion cannot be expected when $\boldsymbol{Da/Ra_D^2 > 2 \text{ x } 10^{-3}}$, where $\boldsymbol{Da}$ is the Damköhler number and $\boldsymbol{Ra_D}$ is the Darcy-Rayleigh number. The present problem by Andres and Cardoso [24, 25] was analyzed most recently by Ward et al. [26], they found out the critical Rayleigh number below which the convective motion cannot be expected in the steady state situation. This was referred to as the steady-state no-flow limit. They showed that for the case of $\boldsymbol{Da/Ra_D^2 > 2.5 \text{ x } 10^{-3}}$, no convective motion can be expected. By observation, this value is slightly different from the value gotten by Andres and Cardoso [24, 25] in their analysis.

We focus the present study on theoretical investigations of the onset of Rayleigh-Benard convection in CO_2 sequestration in the anisotropic porous medium within Eastern Niger Delta region with temperature gradient and first-order chemical reaction. Furthermore, we discuss linear stability theory and study the onset of stationary convection in the system, discussing the results obtained in details.

2. Mathematical Formulation of the Problem

Let us consider a heterogeneous anisotropic porous medium with a physical simplified model and coordinate system as that seen in **Figure 1**, whose solute and thermal diffusivities do not have the same value when measured in different directions both vertically and horizontally, with a first order reaction occurring between a dissolved specie (aqueous CO_2) and a chemical specie in the porous matrix (rock). The governing equation assumed to govern the fluid motion in the horizontal porous layer is the Darcy equation with effective variable permeability **K**, assuming that in the formation, permeability decreases with depth and its space variations are modeled by assuming that $\boldsymbol{K = K_0 S(z)}$, where K_0 is the reference permeability and $S(z) = 1 + \lambda z$ represents the dimensionless relative permeability variation in the z-direction alongside several other parameters mentioned which can generate the development of temperature gradient and transfer heat between the warm rock and cold region.

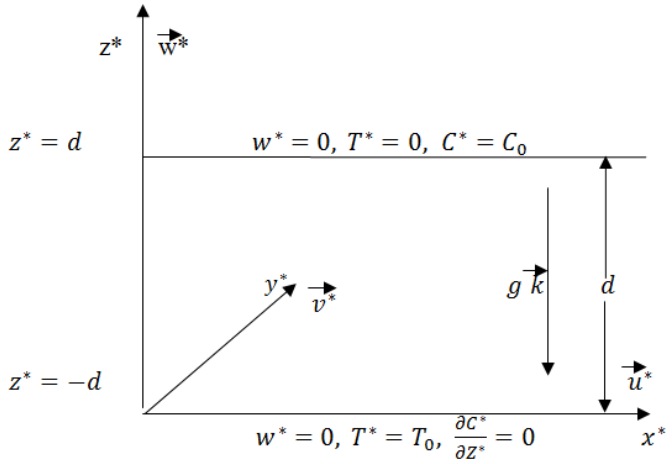

Figure 1: A schematics of the physical simplified model and the coordinate system

For the purpose of this work, we will be considering arbitrary depths (z) from -1 (lower boundary) to 1(upper boundary) since the structure and depth of a deep saline aquifer is not well known. Also arbitrary temperatures will be considered as 0 at the upper boundary the region of lower temperature and 1 at the lower boundary the region of higher temperature. The concentration level of the injected CO_2 will be considered as 1 at the upper boundary just when convection sets in and no flux of solute at the lower boundary will be considered as 0. The relative permeability, $S(z)$ used is a dimensionless parameter which is the ratio of effective variable permeability to reference permeability (absolute permeability of air) varying between 0 and 1, in correlation to the work on Principles of Applied Reservoir Simulation by Fanchi [27]. In this work, the relative permeability

will be considered as $S(z) = 1 + \lambda z$ which represents the dimensionless permeability variation in the z-direction by Hill and Morad [28] and λ will be considered as permeability variability between 0.1 (low permeability region) and 0.9 (high permeability region).

If the horizontal fluid saturated porous layer confined between two parallel boundaries located at $z^* = -d$ and $z^* = d$ is presumed to have an impervious lower boundary with a poorly or perfectly permeable (one-sided model) upper boundary, then the equation of motion for the velocity vector fluid, $\boldsymbol{U}^*$with temperature, T^* and T_0 $(T_0 > T^*)$ and the solute (CO_2) concentration $C^*$and C_0 are represented below with boundary conditions.

$$\boldsymbol{\nabla}^*.\mathbf{U}^* = 0 \tag{1}$$

$$\frac{\mu}{K(z^*)}\mathbf{U}^* = -\boldsymbol{\nabla}^* P^* - \rho(C^*, T^*)g\boldsymbol{k} \tag{2}$$

Where $\boldsymbol{K}$ is the effective variable permeability, μ is the fluid viscosity, $\boldsymbol{k} = (0,0,1)$, P* is the pressure, g is the acceleration due to gravity, ρ is the fluid density and the transport Darcy velocity is $\mathbf{U}^* = (u^*, v^*, w^*)$ along the x, y and z-axis.

Making a Boussinesq approximation, the density variations are assumed to have a fixed part and another part has a linear dependence on temperature and concentration of solute as shown

$$\rho = \rho_0[1 + \beta_C \Delta C^*] \tag{3a}$$

and

$$\rho = \rho_0\,[1 - \beta_T \Delta T^*] \tag{3b}$$

Thus we take the density of solute concentration and temperature to be given by:

$$\rho(C^*, T^*) = \rho_0[\,1 + \beta_C(C^* - C_0) - \beta_T(T^* - T_0)] \tag{3c}$$

The coefficient β_T is expected to be negative, while βc is positive. The static stability of the system is hence known by the signs of $\beta_T(T^* - T_0)$ and $\beta_C(C^* - C_0)$. If either of these is positive, it shows a destabilizing condition, while if it is negative, it shows a stabilizing condition. By substituting the density value $\rho(C^*, T^*)$into the Darcy equation for variable permeability, it yields:

$$\frac{\mu}{K(z^*)}\mathbf{U}^* = -\boldsymbol{\nabla}^* P^* - g\boldsymbol{k}\rho_0[\,1 + \beta_C(C^* - C_0) - \beta_T(T^* - T_0)] \tag{4a}$$

Substituting$P_0^* = P^* - g\boldsymbol{k}\rho_0$which is the reduced pressure field obtained by eliminating hydrostatic pressure from the local pressureP^*, into the above equation to reduce it to

$$\frac{\mu}{K(z^*)}\mathbf{U}^* = -\boldsymbol{\nabla}^* P_0^* + g\boldsymbol{k}\rho_0[\beta_T(T^* - T_0) - \beta_C(C^* - C_0)] \tag{4b}$$

The transport of heat and solute in the anisotropic porous medium is described by the energy equations as shown:

$$\frac{1}{\kappa_z}\left[\gamma\frac{\partial T^*}{\partial t^*} + (\boldsymbol{\nabla}^*.\mathbf{U}^*)T^*\right] = \xi\frac{\kappa_T}{(\rho C_P)_f}\left(\frac{\partial^2 T^*}{\partial x^{*2}} + \frac{\partial^2 T^*}{\partial y^{*2}}\right) + \frac{\kappa_T}{(\rho C_P)_f}\left(\frac{\partial^2 T^*}{\partial z^{*2}}\right) \tag{5}$$

$$\frac{1}{\kappa_z}\left[\phi'\frac{\partial C^*}{\partial t^*} + (\boldsymbol{\nabla}^*.\mathbf{U}^*)C^*\right] = \phi'\kappa_C\xi\left(\frac{\partial^2 C^*}{\partial x^{*2}} + \frac{\partial^2 C^*}{\partial y^{*2}}\right) + \phi'\kappa_C\left(\frac{\partial^2 C^*}{\partial z^{*2}}\right) - \frac{k_r}{\kappa_z}aC^* - C_0 \tag{6}$$

Here, T^* represents the temperature and C^* the concentration of solute in the fluid. κ_C is the solute diffusivity while κ_T is the thermal diffusivity and $\alpha_T = \frac{\kappa_T}{(\rho C_p)_f}$ is the thermal diffusivity through the fluid. γ is the ratio of heat capacities and can be written as $\gamma = \frac{(\rho C_P)_m}{(\rho C_P)_f}$, where $(\rho C_P)_m$is noted as the volumetric heat capacity of the saturated medium while $(\rho C_P)_f$is the volumetric heat capacity of the fluid. $\phi'$is the porosity of the matrix and $k_r a$is the reaction rate constant based on the solid surface area per unit volume of the porous medium. β_T and $\beta_C$are the thermal and solutal expansion coefficient respectively, while T_0 and $C_0$are the reference temperature and concentration of CO_2 respectively.

If the solute concentration is maintained at the upper boundary, then we express it as $C^* = C_0$ at $z^* = d$. If the flux of CO_2 is set to zero at the lower boundary, then we express this condition as $\frac{\partial C^*}{\partial z^*} = 0$ at $z^* = 0$. The majority of studies have considered the one-sided model where $C = C_0$ at the upper boundary and $\frac{\partial C}{\partial z} = 0$ at the lower boundary. This indicates that two cases are considered for the boundary conditions, namely an impervious lower boundary with either a permeable or poorly permeable upper boundary and thus the boundary conditions were derived by taking the solute concentration to be constant at the upper boundary while temperature is constant at the lower boundary and there is no flux of solute across the lower boundary. Thus the boundary conditions are;

$$w^* = 0, T^* = 0 \text{ and } C^* = C_0 \text{ at} z^* = d \quad (7a)$$

$$w^* = 0, T^* = T_0 \text{ and } \frac{\partial C^*}{\partial z^*} = 0 \text{ at } z^* = -d \quad (7b)$$

2.1. Non-dimensionalization

We defined the dimensionless variables by;

$$x^* = dx,\ y^* = dy,\ z^* = dz \quad (8a)$$

$$u^* = \frac{\kappa_z \alpha_T u}{d},\ v^* = \frac{\kappa_z \alpha_T v}{d},\ w^* = \frac{\kappa_z \alpha_T w}{d},\ t^* = \frac{d^2 \Upsilon t}{\kappa_z \alpha_T} \quad (8b)$$

$$T^* = T_0 + T\Delta T,\ C^* = C_0 + C\Delta C \quad (8c)$$

$$\boldsymbol{\nabla}^* = \frac{1}{d}\boldsymbol{\nabla}, \boldsymbol{\nabla}^{*2} = \frac{1}{d^2}\boldsymbol{\nabla}^2 \quad (8d)$$

With the defined dimensionless variables in Eqs. (8a) - (8d), all equations pointed out in previous discussions from Eqs (1, 4b, 5 and 6) respectively will be non-dimensionalized to obtain:

$$\boldsymbol{\nabla}.\boldsymbol{U} = 0 \quad (9)$$

$$\frac{\boldsymbol{U}}{S(z)} = -\boldsymbol{\nabla}P + RaT\boldsymbol{k} - RsC\boldsymbol{k} \quad (10)$$

Where Ra = thermal Rayleigh number $= \frac{\rho_0 g \beta_T d^2 K_0(\Delta T)}{\mu \kappa_z \alpha_T}$

Rs = Solutal Rayleigh number $= \frac{\rho_0 g \beta_C d^2 K_0(\Delta C)}{\mu \kappa_z \alpha_T}$

$P = \frac{K_0 d P_o^*}{\mu \kappa_z \alpha_T}$

$K(z) = K_0 S(z)$

$S(z) = 1 + \lambda z$ which represents the dimensionless permeability variation in the z-direction.

$$\left[\frac{\partial T}{\partial t} + (\boldsymbol{\nabla}.\boldsymbol{U})T\right] = \xi\left(\frac{\partial^2 T}{\partial x^2} + \frac{\partial^2 T}{\partial y^2}\right) + \left(\frac{\partial^2 T}{\partial z^2}\right) \quad (11)$$

and

$$\phi\frac{\partial C}{\partial t} + (\boldsymbol{\nabla}.\boldsymbol{U})C] = \frac{1}{Le}[\xi\left(\frac{\partial^2 C}{\partial x^2} + \frac{\partial^2 C}{\partial y^2}\right) + \left(\frac{\partial^2 C}{\partial z^2}\right)] - DaC \quad (12)$$

Where Da = Damköhler number (the ratio of solute reaction to diffusion rates) $= \frac{k_r a d^2}{\kappa_z \alpha_T}$

α_T =Thermal diffusivity through the fluid = $\frac{\kappa_T}{(\rho C_p)_f}$

Le = Lewis number, the ratio of thermal diffusivity to mass diffusivity = $\frac{\alpha_T}{\phi' \kappa_C}$

ϕ = The dimensionless porosity = $\frac{\phi'}{\gamma}$

ξ = The ratio of the horizontal to the vertical solutal and thermal diffusivities = $\frac{\kappa_h}{\kappa_z}$

With boundary conditions:

$$w = 0, T = 0, C = 1 \, at \, z = 1 \quad (13a)$$

$$w = 0, T = 1, \frac{\partial C}{\partial z} = 0 at \, z = -1 \quad (13b)$$

2.2. Basic Steady-State Motionless Condition

Here, we assume a physical situation were a fixed amount of supercritical carbon dioxide has been injected through the top boundary for a short time and then the injection is stopped. This forms a thick carbon-rich brine layer on top an impermeable carbon-free and lighter brine layer. Therefore, the motionless or diffusive base state of the concentration profile and its basic state temperature in isotropic porous medium is mathematically determined using the **WOLFRAM MATHEMATICA 11.1 SOFTWARE**. By considering the following dimensionless boundary conditions, the base state is modelled thus:

$\boldsymbol{U} = \boldsymbol{U_b}(z),\ P = P_b(z),\ T = T_b(z),\ C = C_b(z)$ and $\boldsymbol{U}_b \longrightarrow 0, \frac{\partial}{\partial t} \rightarrow 0$ for the motionless case and Eqs. (10) – (12) becomes

$$\frac{dP_b}{dz} = RaT_b(z) - RsC_b(z) \quad (14)$$

$$\frac{d^2 T_b}{dz^2} = 0 \quad (15)$$

and $\frac{d^2C_b}{dz^2} - LeDaC_b = 0$ (16)

with boundary conditions;

$\frac{\partial C_b}{\partial z} = 0$ and $T_b = 0$ at $z = 1$ (17a)

$C_b = 1$ and $T_b = 1$ at $z = -1$ (17b)

It is important to note that the fluid layer will remain at rest (its basic steady state) while the stabilizing processes dominates until perturbation sets in due to difference in densities caused by temperature difference, were the top temperature is lower than the bottom temperature and the carbon-rich layer at the surface is denser than its new surroundings. Thus, it will sink back down allowing convection to set in. Using the boundary conditions in Eqs. (17a) and (17b) and the Wolfram Mathematica 11.1 software, we obtain the values of the basic state concentration, $C_b(z)$ and temperature, $T_b(z)$ as;

$C_b(z) = cosh\,[\sqrt{Da}\sqrt{Le}\,(1-z)]\;sech\,[2\sqrt{Da}\sqrt{Le}]$ (18)

and $T_b(z) = 1 - z$ (19)

At the basic steady state, the temperature is a linear temperature distribution and as such the distribution is based on the fact that the geothermal gradient is constant in the subsurface formation, in the fluid and rock matrix. This means that the top and bottom surfaces are constant.

2.3. Perturbation of the Basic Steady-State

As perturbation sets in due to difference in densities caused by an increase in the geothermal gradient (a higher temperature at the lower boundary than at the top boundary) between an unstable thick carbon-rich layer over a carbon-free layer, buoyancy diffusion in the unstably stratified state causes the carbon-rich layer to allow convection set in as long as a certain thickness of the boundary layer is not exceeded or critical concentration difference has not been established, otherwise the layer prevents convection from setting it. The concentration, temperature, pressure and velocity components in the z-direction are subjected to infinitesimal perturbations. To study the stability of the basic steady-state, we superimpose perturbations on the basic steady-state such that $U = 0 + u$, $T = T_b(z) + \theta, C = C_b(z) + c$ and $P = P_b(z) + p$. Where $\theta << T_b(z)$, $c << C_b(z)$ and $p << P_b(z)$. If the perturbation quantities are used in Eqs. (9) – (12) for dimensionless velocity perturbations, dimensionless perturbed pressure, dimensionless perturbed temperature and dimensionless perturbed concentration respectively neglecting all higher order nonlinear terms, the following equations are derived;

$\boldsymbol{\nabla} . \boldsymbol{u} = 0$ (20)

$\frac{\mathbf{u}}{S(z)} = -\boldsymbol{\nabla} p + Ra\theta\boldsymbol{k} - Rsc\boldsymbol{k}$ (21)

$\left[\frac{\partial\theta}{\partial t} + w\frac{dT_b(z)}{dz} + (\boldsymbol{\nabla} . \boldsymbol{u})\theta\right] = \xi\left(\frac{\partial^2\theta}{\partial x^2} + \frac{\partial^2\theta}{\partial y^2}\right) + \left(\frac{\partial^2\theta}{\partial z^2}\right)$ (22)

$\left[\phi\frac{\partial c}{\partial t} + w\frac{dC_b(z)}{dz} + (\boldsymbol{\nabla} . \mathbf{u})\mathrm{c}\right] = \frac{1}{Le}\left[\xi\left(\frac{\partial^2 c}{\partial x^2} + \frac{\partial^2 c}{\partial y^2}\right) + \left(\frac{\partial^2 c}{\partial z^2}\right)\right] - Dac$ (23)

The resulting equations are called linearized equations. This shows that perturbation leads to linearization. The boundary conditions are:

$\theta = 0, c = 0$ and $w = 0\; at\; z = -1$ (24a)

$\theta = 0, \frac{\partial c}{\partial z} = 0$ and $w = 0\; at\; z = 1$ (24b)

However, fixed temperature gradients are used for the top and bottom boundaries and for the entire aquifer layer while a transient state is assumed for the concentration.

3. Linear Stability Analysis

To understand the processes occurring during carbon dioxide sequestration in underground saline aquifers, it is important to assess the onset of convection (instability in the system). The linear stability analysis conducted is to determine the minimum or critical Rayleigh number after which buoyancy-driven flow of the fluid begins to occur. In this section, we use the linear theory to predict the thresholds for marginal or stationary convection modes in anisotropic porous medium. To proceed with the linear stability analysis, we seek Fourier mode solutions defined by Eqs (25a) – (25c) below subject to boundary conditions same as in Eqs (24a) and (24b).

$w = w_0 \sin \pi z e^{i(a_x x + a_y y)} e^{\sigma t}$ (25a)

$$\theta = \theta_0 \sin \pi z e^{i(a_x x + a_y y)} e^{\sigma t} \quad (25b)$$

$$c = c_0 \sin \pi z e^{i(a_x x + a_y y)} e^{\sigma t} \quad (25c)$$

Where a_x is the wave number in the x-direction, a_y is the wave number in the y-direction and σ is the growth rate of the disturbances. The functions w_0, θ_0 and c_0 satisfies the boundary conditions same as in Eqs (24a) and (24b). Assuming that the disturbance quantities (amplitudes of the perturbations to the base state) are small and thus their non-linear products are neglected. The pressure term in Eq (21) can be eliminated by operating double curl on the momentum equation (Eq 21) and considering quantities in the z-plane only (unit vector $\boldsymbol{k}$) and this gives;

$$\frac{1}{S(z)}\left[\frac{\partial^2}{\partial x^2} + \frac{\partial^2}{\partial y^2} + \frac{\partial^2}{\partial z^2}\right] w = Ra\left(\frac{\partial^2 \theta}{\partial x^2} + \frac{\partial^2 \theta}{\partial y^2}\right) - Rs\left(\frac{\partial^2 c}{\partial x^2} + \frac{\partial^2 c}{\partial y^2}\right) \quad (26)$$

By neglecting the non-linear products in Eqs (22) and (23) we obtain the linearized version of the dimensionless perturbed temperature and concentration equation as shown in Eqs (27) and (28);

$$\left[\frac{\partial \theta}{\partial t} - w\right] = \xi\left(\frac{\partial^2 \theta}{\partial x^2} + \frac{\partial^2 \theta}{\partial y^2}\right) + \left(\frac{\partial^2 \theta}{\partial z^2}\right) \quad (27)$$

$$\left[\phi \frac{\partial c}{\partial t} + wf(z)\right] = \frac{1}{Le}\left[\xi\left(\frac{\partial^2 c}{\partial x^2} + \frac{\partial^2 c}{\partial y^2}\right) + \left(\frac{\partial^2 c}{\partial z^2}\right)\right] - Dac \quad (28)$$

Where $T_b(z) = 1 - z$, and $\frac{dC_b}{dz} = f(z) = -\sqrt{DaLe}\,\text{sech}\left(2\sqrt{DaLe}\right)\sinh\left(\sqrt{DaLe}(1-z)\right)$

The resulting Eqs (26), (27) and (28) are solved using time-dependent periodic disturbances in a horizontal plane by substituting the Fourier mode solutions, Eqs (25a) – (25c) into the momentum equation and the linearized version of the perturbed temperature and concentration equations. Where a_x and a_y are horizontal wavenumbers and σ is the growth rate, we obtain;

$$\frac{1}{S(z)}[a^2 + \pi^2]w_0 - Ra\, a^2\theta_0 + Rs\, a^2 c_0 = 0 \quad (29)$$

$$-w_0 + (\sigma + \xi a^2 + \pi^2)\theta_0 = 0 \quad (30)$$

$$Lef(z)w_0 + (Le\phi\sigma + \xi a^2 + \pi^2 + LeDa)c_0 = 0 \quad (31)$$

Eqs. (29) – (31) can also be represented in matrix form as AZ = 0, where;

$$\text{A} = \begin{pmatrix} \frac{a^2+\pi^2}{S(z)} & -Ra\, a^2 & Rs\, a^2 \\ -1 & \sigma + \xi a^2 + \pi^2 & 0 \\ Lef(z) & 0 & Le\phi\sigma + \xi a^2 + \pi^2 + LeDa \end{pmatrix} \quad (32)$$

and $Z = (w_0, \theta_0, c_0)$. By taking $a^2 + \pi^2 = \delta^2$,we have a new equation written in the form AZ =0;

$$\begin{pmatrix} \frac{\delta^2}{S(z)} & -Ra\, a^2 & Rs\, a^2 \\ -1 & \sigma + \xi a^2 + \pi^2 & 0 \\ Lef(z) & 0 & Le\phi\sigma + \xi a^2 + \pi^2 + LeDa \end{pmatrix} \begin{pmatrix} w_0 \\ \theta_0 \\ c_0 \end{pmatrix} = 0 \quad (33)$$

The solvability of Eq (33) requires that the determinant $/A/$ must vanish and $/A/ = 0$. This will yield an expression for the Rayleigh number Ra as;

$$Ra = \frac{(\delta_1^2 + \sigma)(LeDa + Le\phi\sigma + \delta_1^2)\delta^2 - Rs\, a^2 S(z) f(z) Le(\delta_1^2 + \sigma)}{a^2 S(z)(LeDa + \delta_1^2 + Le\phi\sigma)} \quad (34)$$

Where $\delta^2 = a^2 + \pi^2$

and $\delta_1^2 = \xi a^2 + \pi^2$

By considering $\sigma = i\omega$ in Eq. (34), we obtain the real and imaginary parts of Ra and thus

$$Ra = Ra_{real} + Ra_{imag} \quad (35)$$

We now take the conjugate of Eq. (34) and the real part of Ra becomes;

$$Ra_{real} = \frac{\delta^2[\delta_1^4(\xi a^2 + \pi^2) + Le\phi\,\omega^2(Le\delta_1^2\phi - \delta_1^2 + \xi a^2 + \pi^2)] + LeDa\,\delta_1^2\delta^2(LeDa + \xi a^2 + \pi^2 + \delta_1^2) - Rs\, a^2 S(z) f(z) Le(LeDa\,\delta_1^2 + \delta_1^4 + Le\phi\,\omega^2)}{a^2 S(z)(Le^2 Da^2 + 2LeDa\,\delta_1^2 + \delta_1^4 + Le^2\omega^2\phi^2)} \quad (36)$$

While the imaginary part of Ra becomes;

$$Ra_{imag} = \frac{\delta^2[Le\phi(Le\phi\,\omega^2 - \delta_1^2\xi a^2 - \delta_1^2\pi^2 + \delta_1^4) + \delta_1^2(\xi a^2 + \pi^2) + LeDa(LeDa + \xi a^2 + \pi^2 + \delta_1^2)] + RsS(z)a^2 f(z) Le(Le\phi\,\delta_1^2 - \delta_1^2 - LeDa)}{a^2 S(z)(Le^2 Da^2 + 2LeDa\,\delta_1^2 + \delta_1^4 + Le^2\omega^2\phi^2)} \quad (37)$$

3.1. Stationary Convection

For the onset of stationary convection, set $\omega = 0$ in the real part of Ra in Eq. (36) for the validity of principle of exchange of stabilities (steady case). The Rayleigh number at which marginally stable steady mode exists becomes;

$$Ra^{(s)} = \frac{\delta_1^2[\delta^2(\delta_1^2+LeDa)-RsS(z)f(z)a^2Le]}{a^2S(z)(\delta_1^2+LeDa)} \tag{38}$$

Now we compute the critical (minimum) value of the critical wave number, a_c and the corresponding critical Rayleigh number, $Ra_c^{(s)}$ for the onset of convection. By setting $a = a_c$ in Eq. (38) and minimize according to the condition

$$\frac{\partial Ra^{(s)}}{\partial a_c^2} = 0 \tag{39}$$

This yields;

$$\frac{-\pi^4S(z)(Da+Le^{-1}\pi^2+Le^{-1}a^2\xi)^2+\xi a^4S(z)(Da+Le^{-1}\pi^2+Le^{-1}a^2\xi)^2-\xi Daf(z)a^4RsS(z)^2}{a^4S(z)^2(Da+Le^{-1}\pi^2+Le^{-1}a^2\xi)^2} = 0 \tag{40}$$

By expansion and simplification;

$$a^8(\xi^3) + a^6(2DaLe\xi^2 + 2\pi^2\xi^2) + a^4(Da^2Le^2\xi + 2DaLe\pi^2\xi + \pi^4\xi - \pi^4\xi^2 - DaLe^2f(z)RsS(z)\xi) - a^2(2DaLe\pi^4\xi + 2\pi^6\xi) - a^0(Da^2Le^2\pi^4 + 2DaLe\pi^6 + \pi^8) = 0 \tag{41}$$

Which satisfies a polynomial equation;

$$x_8a^8 + x_6a^6 + x_4a^4 - x_2a^2 - x_0 = 0 \tag{42}$$

Where $x_8 = 1$

$$x_6 = 2DaLe\xi^2 + 2\pi^2\xi^2$$
$$x_4 = Da^2Le^2\xi + 2DaLe\pi^2\xi + \pi^4\xi - \pi^4\xi^2 - DaLe^2f(z)RsS(z)\xi$$
$$x_2 = 2DaLe\pi^4\xi + 2\pi^6\xi$$
$$x_0 = Da^2Le^2\pi^4 + 2DaLe\pi^6 + \pi^8$$

3.2. Solutions for Marginal/Stationary State Convection Modes in Anisotropic Medium

It is necessary to obtain a 2D contour plot and 3D plot to produce horizontal convective rolls (long rolls of counter – rotating air usually caused by convection) indicating the onset of instability in the stationary convective mode in the anisotropic medium, through flow patterns between two large parallel plates. The change in density mentioned in previous section is due to temperature variations giving rise to convective rolls. Although the motion is usually opposed by the viscous forces in the fluid, a balance between the forces will indicate through convective rolls, the onset of instability in poor or low permeability areas and high permeability areas. The marginal/stationary steady state mode makes use of the minimum/critical Rayleigh number obtained via linear stability analysis to determine at what critical depth does convection first occurs. This is achieved by obtaining the real part of w, θ and c from the Fourier mode solutions obtained for the anisotropic medium in Eqs. (25a) - (25c) by first minimizing and taking the wavenumber $a = 1$, the growth rate $\sigma = 0$ and $\theta_0 = 1$ in Eq. (30) to obtain w_0 as seen below;

$$w_0 = (\xi + \pi^2) \tag{43}$$

Substituting Eq. (43) in Eq. (31) to obtain

Thus; $$c_0 = \frac{-Lef(z)(\xi+\pi^2)}{LeDa + (\xi+\pi^2)} \tag{44}$$

Substitute $\theta_0 = 1$, $k = 1$ and Eq. (44) into Eq. (29) to obtain w_0

$$w_0 = \frac{S(z)}{(1+\pi^2)}\left[Ra + Rs\frac{Lef(z)(\xi+\pi^2)}{LeDa + (\xi+\pi^2)}\right] \tag{45}$$

Substitute Eq. (45) into Eq. (25a) to obtain w

$$w = \left[\frac{S(z)}{1+\pi^2}Ra + \frac{S(z)}{(1+\pi^2)}\frac{RsLef(z)(\xi+\pi^2)}{LeDa + (\xi+\pi^2)}\right][\sin(\pi z)\cos(x)\cos(y) + \sin(\pi z)isin(y)\cos(x) + \sin\pi zisinxcosy - \sin\pi z\sin x\sin y \tag{46}$$

By expanding Eq. (46), we obtain real and imaginary parts of the equation of which the real part of w is most useful in obtaining 2D contour plots and 3D plots for the stationary convection modes in the anisotropic porous medium as seen in the next section because of the presence of the critical Rayleigh number term.

$$w = \frac{S(z)\sin(\pi z)}{1+\pi^2}\left[Ra_c^{(s)}\cos(x)\cos(y) - Ra_c^{(s)}\sin(x)\sin(y)\right] + \frac{S(z)\sin(\pi z)}{1+\pi^2}\left[\frac{RsLef(z)(\xi+\pi^2)}{LeDa+(\xi+\pi^2)}\cos(x)\cos(y) - RsLefz\xi+\pi 2LeDa+\xi+\pi 2\sin x\sin y\right. \quad (47)$$

Revealed in the results are 2D contour plots and 3D plots to describe the minimum or critical depth a medium already injected with CO_2 will remain stable before the onset of convection begins to manifests in the stationary convective mode through horizontal convective rolls (long rolls of counter – rotating air usually caused by convection) in the anisotropic medium.

4. Results and Discussion

The purpose of our investigation has been to study the onset of Rayleigh-Benard convection which is important in CO_2 sequestration in the anisotropic porous medium. In our study, the onset of Rayleigh-Benard convection in CO_2 sequestration in the anisotropic porous medium of the Eastern Niger Delta region as affected by temperature gradient and First-order chemical reaction has been investigated using linear stability analysis. Analytical expressions for the critical Rayleigh number and their corresponding wavenumbers for the onset of stationary convections were determined using linear stability theory. In the analysis of stationary convection, our study shows that the critical Rayleigh number for the onset of convection depends on four parameters the Damköhler number Da, Lewis number Le, the solutal Rayleigh number Rs and λ such that $1+\lambda z$ represents the dimensionless permeability variation in the z-direction. The effects of these parameters on the governing equations are discussed on the basic concentration distribution and on the onset of stationary convections numerically and graphically.

Figure 2 shows the effect of the Damköhler number, Da on the distribution of basic concentration, $C_b(z)$of the system plotted with respect to its depth, z across the fluid layer for fixed values of the Lewis number ($Le = 1$). It is observed that an increase in the solute reaction rate to diffusion rate (Damköhler number), rapidly decreases the concentration level of sequestrated CO_2 at the upper boundary in the system. This thus means that in the presence of perturbation, where heating, chemical reaction and a change in density occurs and increases, the concentration level of the sequestrated CO_2 in turn decreases from the upper boundary. This indicates that increasing Damköhler number, Da has a destabilizing effect to make the system more unstable.

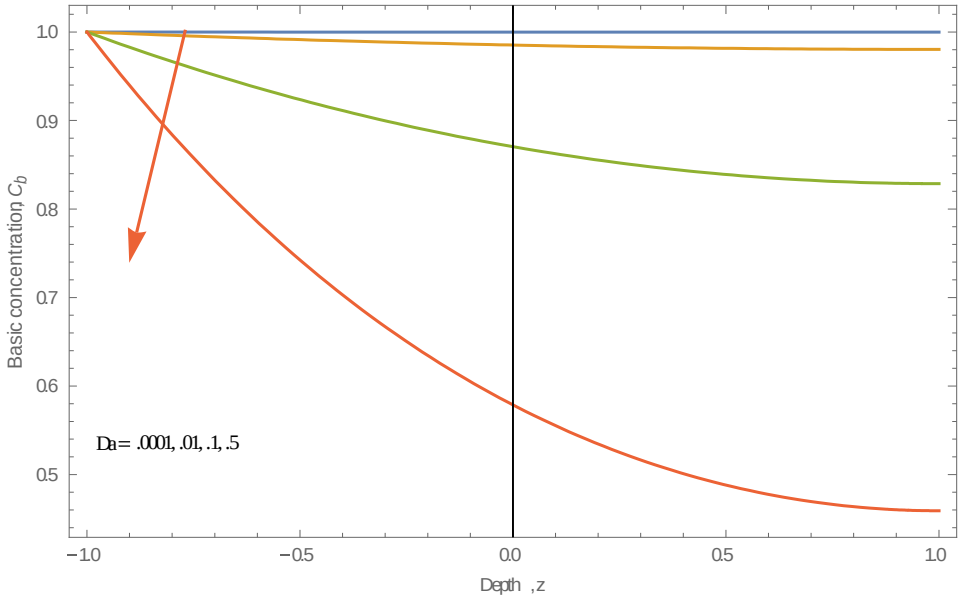

Figure 2: Visual representation of the effect of the Damköhler number, Daon the distribution of basic concentration, $C_b(z)$.

Figure (3a) and (3b) displays the effect of increasing Damköhler number, Da on the curve for stationary convection modes and fixed values of other parameters as $\lambda = 0.1$, $Rs = 10$ and $Le = 1$.A gradual increase in the solute reaction rate to diffusion rate from $Da = 0.1$ to $Da = 0.2$, and in the presence of Lewis number and

Solute Rayleigh number has a significant effect on the instability of the system in the anisotropic porous medium from $\xi > 1$ to $\xi < 1$ at the upper boundary of a region. Even at low permeability, the onset of instability is still facilitated at $\xi < 1$, while there is a rapid delay in the onset of instability in the anisotropic porous medium at $\xi > 1$also at low permeability. This thus means that (with respect to the onset of instability) varying the ratio of horizontal solute and thermal diffusivity to vertical solute and thermal diffusivity does have a significant effect at $\xi < 1$ than at $\xi > 1$even in areas known with low permeability. This therefore means that areas with low permeability will be suitable for CO_2 sequestration as the reaction rate to diffusion rate in the anisotropic porous medium increases.

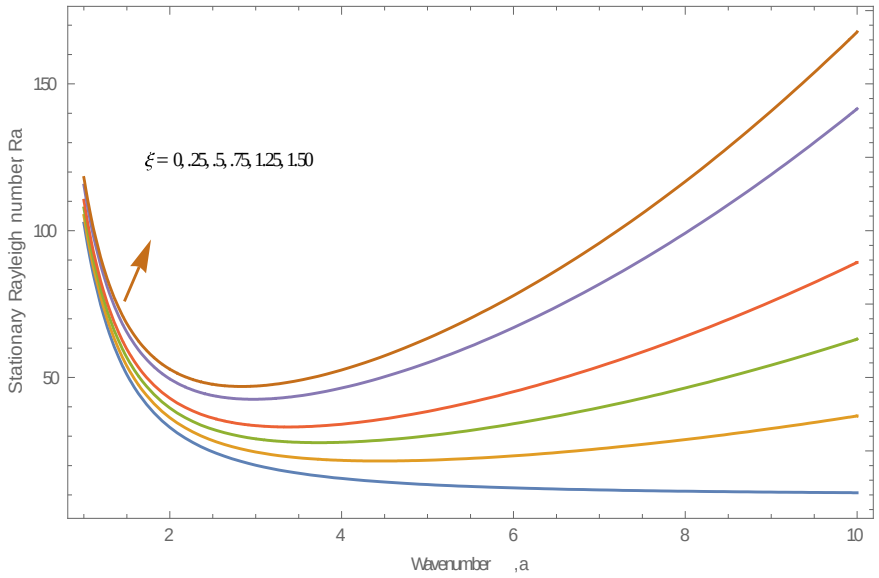

Figure 3a: Plot of the stationary Rayleigh number, $Ra^{(s)}$ with respect to wavenumber, afor increasing values of ξ and fixed values of $Da = 0.1,\ Rs = 10,\ Le = 1,\ \lambda = 0.1$ and $z = 0.5$

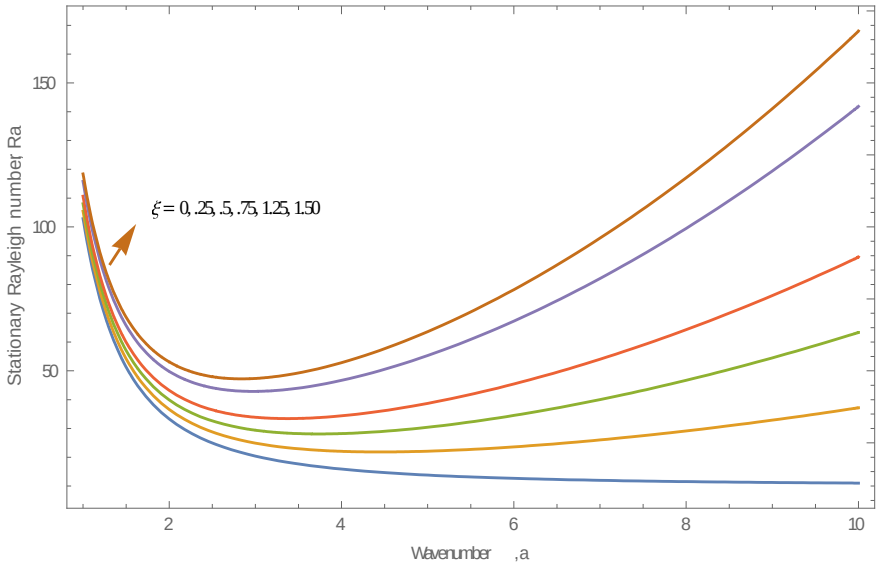

Figure 3b: Plot of the stationary Rayleigh number, $Ra^{(s)}$ with respect to wavenumber, afor increasing values of ξ and fixed values of $Da = 0.2,\ Rs = 10,\ Le = 1,\ \lambda = 0.1$ and $z = 0.5$

Figure (4a) and (4b) displays the effect of increasing Damköhler number, Da on the curve for stationary convection modes and fixed values of other parameters $as\,\lambda = 0.9,\ Rs = 10$ and $Le = 1$. A gradual increase in the solute reaction rate to diffusion rate from $Da = 0.1$ to $Da = 0.2$, and in the presence of Lewis number and Solute Rayleigh number has a significant effect on the instability of the system in the anisotropic porous medium from $\xi > 1$ to $\xi < 1$ at the upper boundary of a region. At high permeability regions, the onset of

instability is very much facilitated at $\xi < 1$, while there is only a slight delay in the onset of instability in the anisotropic porous medium at $\xi > 1$ also at high permeability. This thus means that (with respect to the onset of instability) varying the ratio of horizontal solute and thermal diffusivity to vertical solute and thermal diffusivity does have a significant effect at $\xi < 1$ than at $\xi > 1$ in areas of high permeability. This therefore means that areas with high permeability will be even more suitable for CO_2 sequestration as the reaction rate to diffusion rate in the anisotropic porous medium increases.

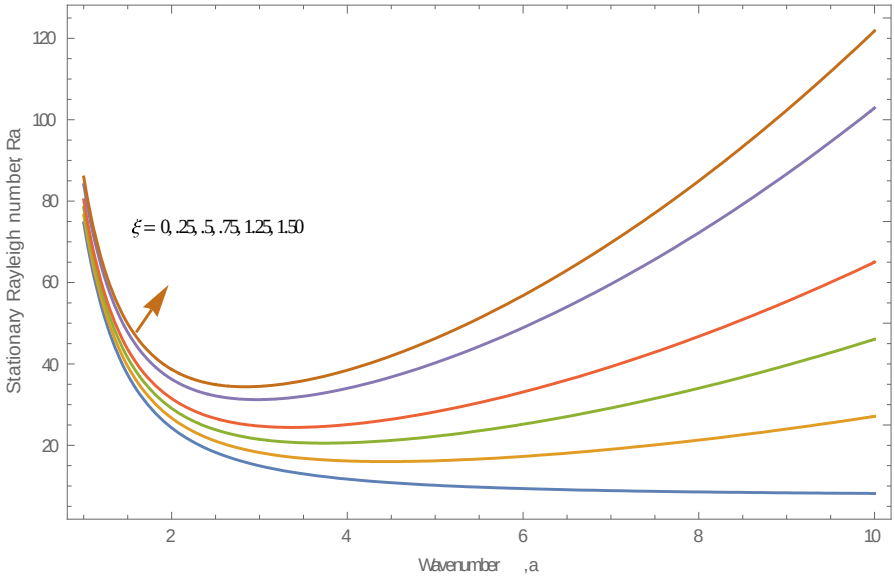

Figure 4a: Plot of the stationary Rayleigh number, $Ra^{(s)}$ with respect to wavenumber, a for increasing values of ξ and fixed values of $Da = 0.1,\ Rs = 10,\ Le = 1,\ \lambda = 0.9$ and $z = 0.5$

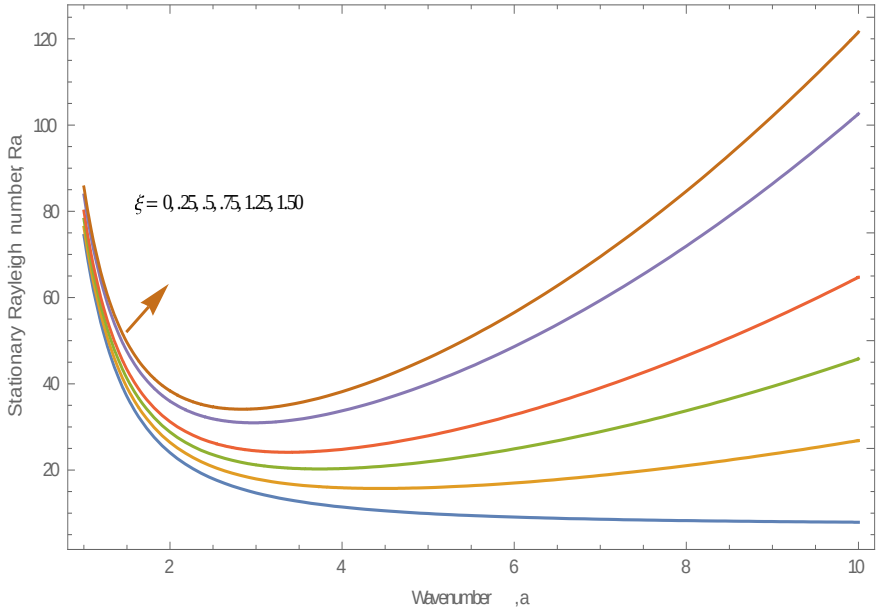

Figure 4b: Plot of the stationary Rayleigh number, $Ra^{(s)}$ with respect to wavenumber, a for increasing values of ξ and fixed values of $Da = 0.2,\ Rs = 10,\ Le = 1,\ \lambda = 0.9$ and $z = 0.5$

Figure (5a) and (5b) displays 2D contour plots of streamlines with varying permeability, λ. A slight increase in permeability causes a significant increase in the onset of instability of the system close to the upper boundary in the anisotropic porous medium. By changing the values of λ from *0.1* to *0.9*, we also change the permeable level of the medium around the carbon dioxide. Where λ is bigger the fluid adjusts itself to the top of the surface than when λ is smaller but, the convection of CO_2 changes, the permeable levels are both strong and CO_2 penetrates

easier in both cases. This is made possible only where $\xi < 1$ (the ratio of horizontal solute and thermal diffusivity to vertical solute and thermal diffusivity), in agreement with the research work by Vo and Hadji [29]. When $\lambda = 0.1$, the center of the streamlines are pronounced at $z_0 = 0.75$ where the blue signifies the light fluid and yellow the heavy fluid. But, an increase in the value of $\lambda = 0.9$, the center of the streamlines are still pronounced and the fluid adjusts itself to the top of the surface almost at $z_0 = 0.8$. Although there is not much difference in the concentration of CO_2 at the different values of λ, but z_0 has a lot of effects on the fluid. In summary, at $\lambda = 0.9$, the critical depth for the onset of convection in the anisotropic porous medium occurs earlier at $z_0 = 0.8$ than at $\lambda = 0.1$, where the onset of instability occurs later at $z_0 = 0.75$ but CO_2 penetrates easily and convection sets in early in both permeability levels but only at $\xi = 0.75,\ 0.50,\ 0.25$. It is important to note that varying the permeability in the vertical direction has no effect on the onset of instability in the system close to the upper boundary this is also in agreement with the work by Hill and Morad [28]. As shown in Figure 5a and 5b, varying the permeability in the vertical direction from $y = 1$ to $y = 20$ had no significant effect on the system close to the top boundary in the anisotropic porous medium.

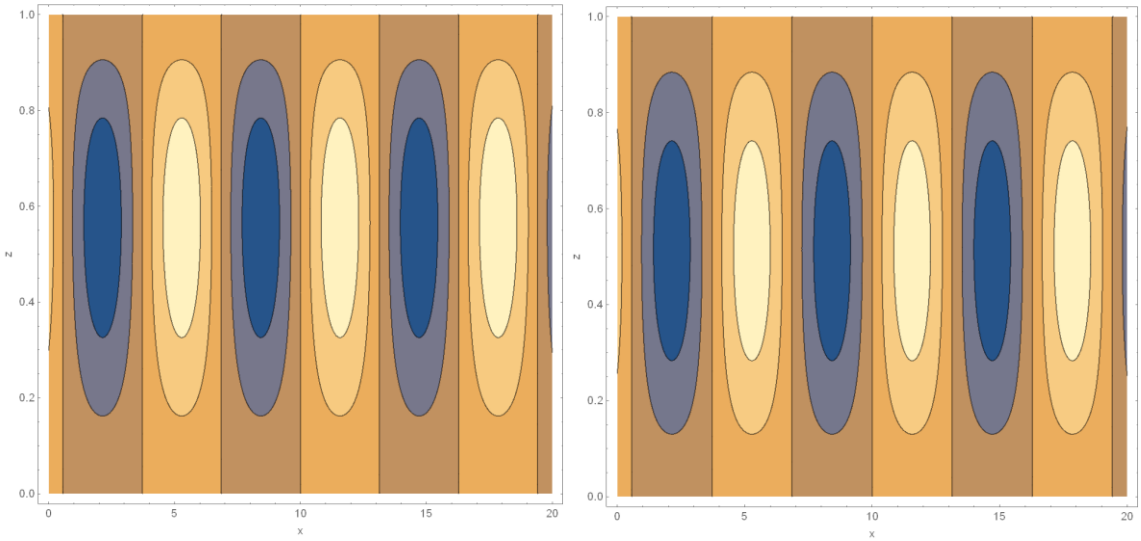

Figure 5a: 2D contour plots of streamlines with varying permeability,λ and fixed values of $Le = 1$, $\xi = 0.50$, $Rs = 10$, and $Da = 0.2$. First: $Ra_c^{(s)} = 20.6244$ at $\lambda = 0.9$; Second: $Ra_c^{(s)} = 28.2152$ at $\lambda = 0.1$and the vertical direction $y = 1$

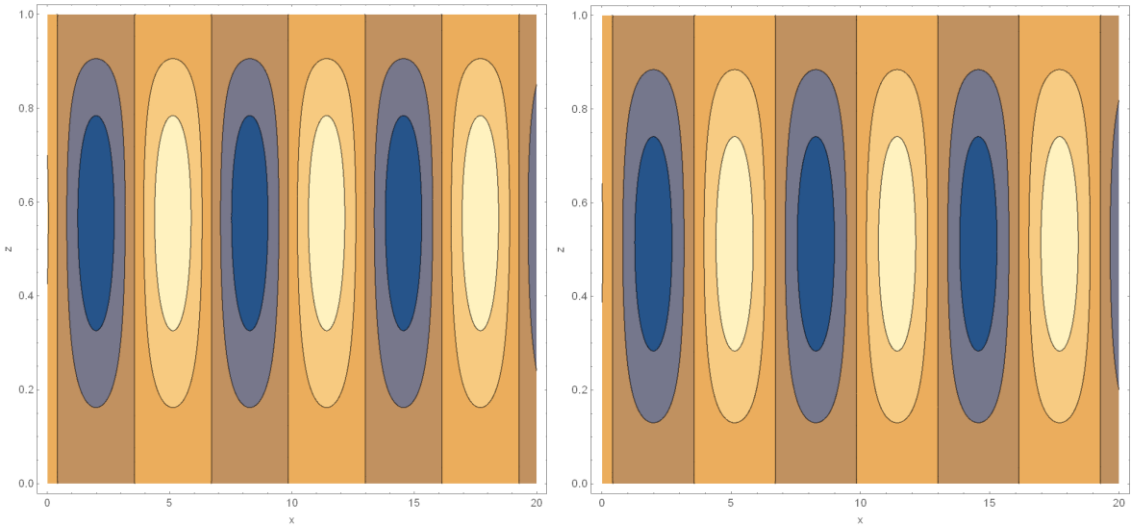

Figure 5b: 2D contour plots of streamlines with varying permeability, λ and fixed values of $Le = 1$, $\xi = 0.50$, $Rs = 10$, and $Da = 0.2$. First: $Ra_c^{(s)} = 20.6244$ at $\lambda = 0.9$; Second: $Ra_c^{(s)} = 28.2152$ at $\lambda = 0.1$ and the vertical direction $y = 20$

Figure 6 and 7 displays 2D contour plots of streamlines with varying reaction rate, Da at $\lambda = 0.1$ and $\lambda = 0.9$ respectively. The size of the convection cell (observe closely the inner convection cell) is increased gradually once reaction rate is increased as the concentration of CO_2 reduces. Physically, reaction rates represent the dissolution of CO_2 into the surrounding brine layer. A more uniform distribution of CO_2 concentration gradient in the domain occurs as a result of CO_2 dissolution taking place as an overall reduction in the overturning motion due to the buoyancy-driven instabilities aided by an increasing reaction rate. Thus in line with Wanstall and Hadji [30], it is proven that reaction rates acts as a dampener for the concentration gradient as shown in Figure 2**.** In the case of the anisotropic porous medium, provided the solute reaction rate dominates the diffusion rate i.e. for higher values of Da, there will always be a reduction in the concentration level of CO_2 regardless of whether there is a significant change in the size of the convection roll.

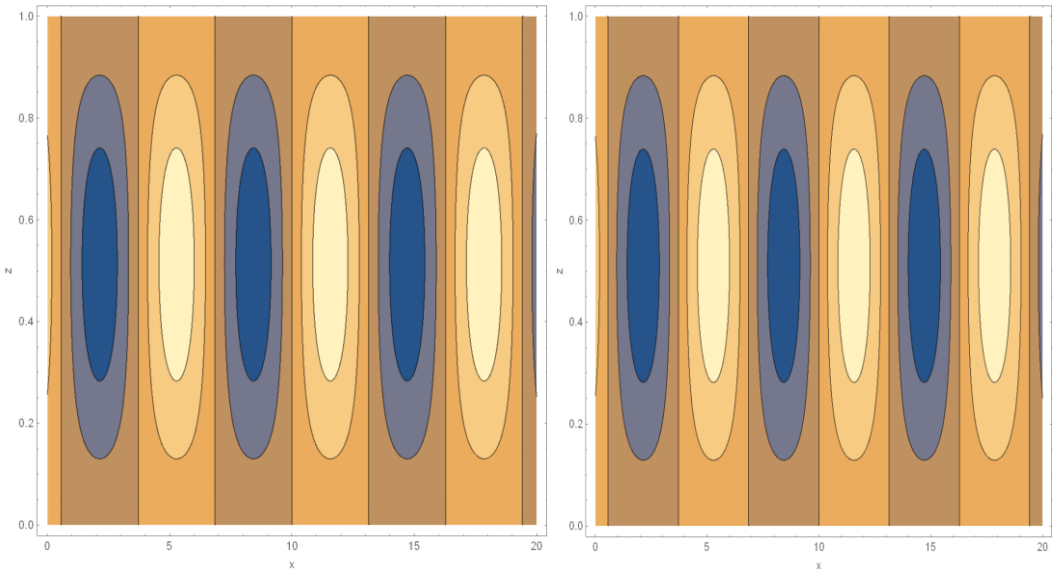

Figure 6a: 2D contour plots of streamlines with varying reaction rate, Da and fixed values of $Le = 1$, $\xi = 0.50$, $Rs = 10$, *and* $\lambda = 0.1$. *First:* $Da = 0.2$ *at* $Ra_c^{(s)} = 28.2152$; *Second* $Da = 0.1$ *at* $Ra_c^{(s)} = 27.9303$ *and the vertical direction at* $y = 1$

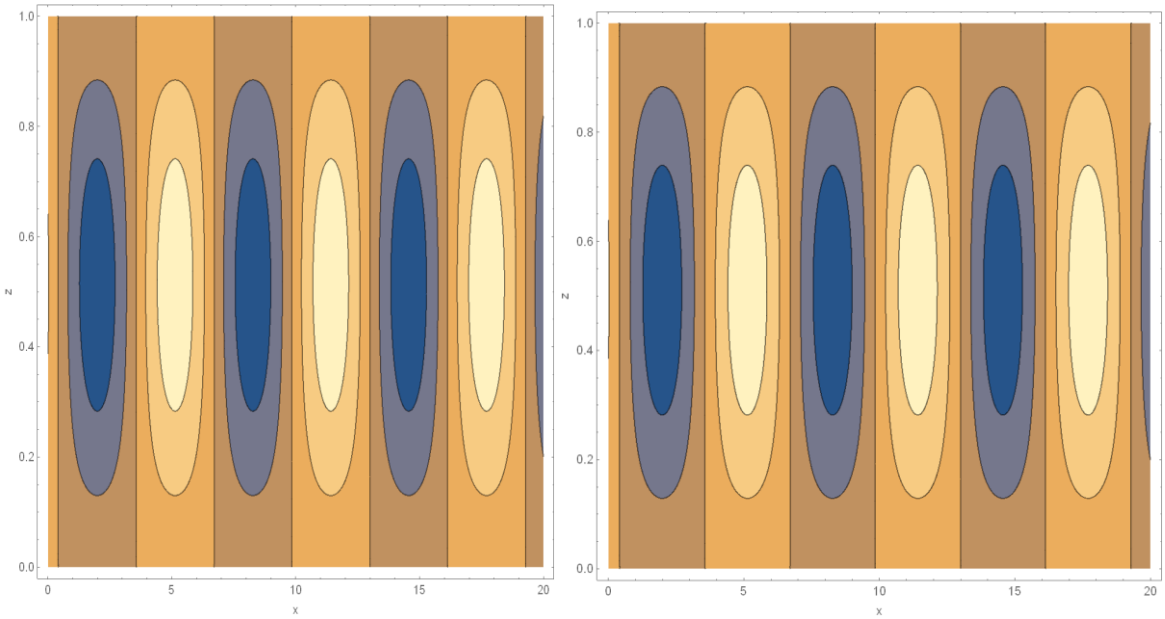

Figure 6b: 2D contour plots of streamlines with varying reaction rate, Da and fixed values of $Le = 1$, $\xi = 0.50$, $Rs = 10$, *and* $\lambda = 0.1$. *First:* $Da = 0.2$ *at* $Ra_c^{(s)} = 28.2152$; *Second* $Da = 0.1$ *at* $Ra_c^{(s)} = 27.9303$ *and the vertical direction at* $y = 20$

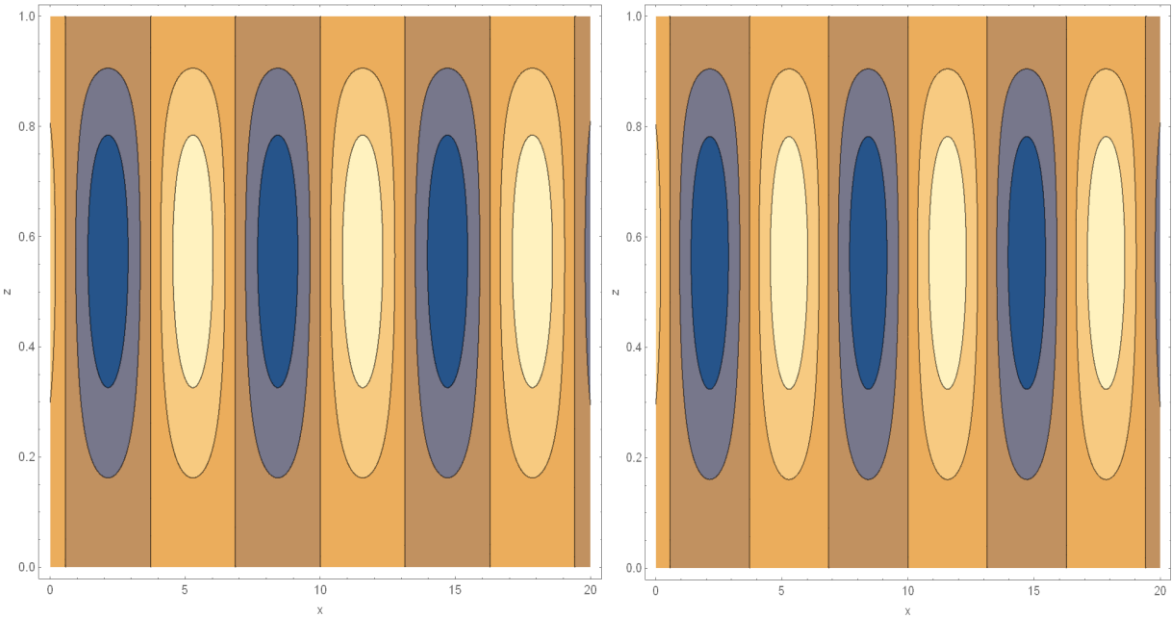

Figure 7a: 2D contour plots of streamlines with varying reaction rate, Da and fixed values of Le = 1, ξ = 0.50, Rs = 10, and λ = 0.9. First: Da = 0.2 at $Ra_c^{(s)} = 20.6422$; Second Da = 0.1 at $Ra_c^{(s)} = 20.3396$ and the vertical direction at y = 1

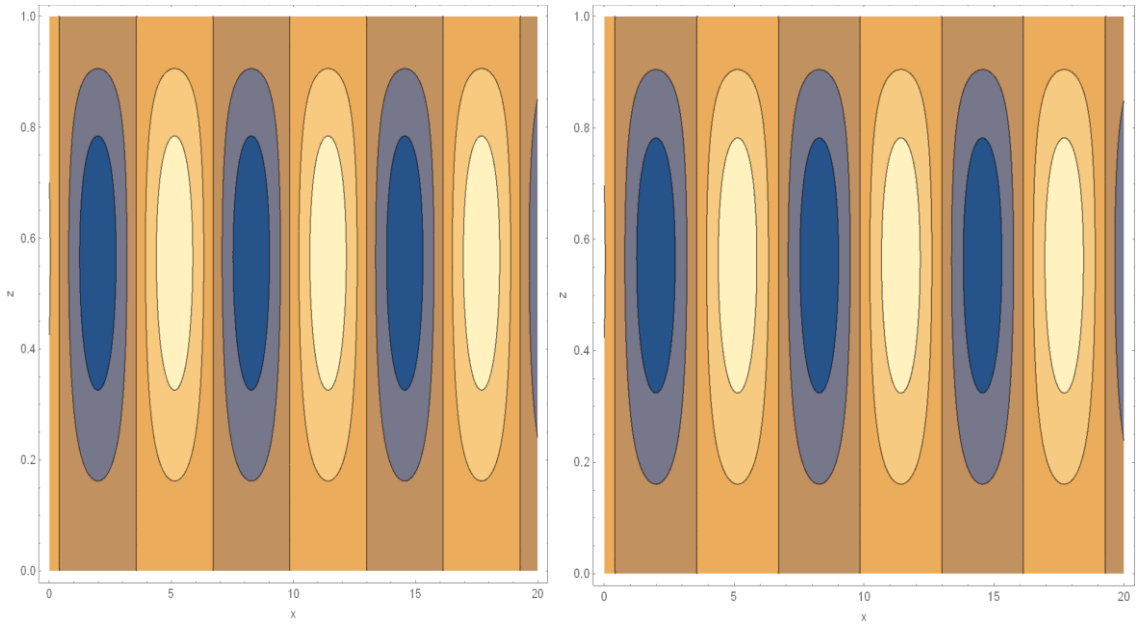

Figure 7b: *2D contour plots of streamlines with varying reaction rate, Da and fixed values of Le = 1, ξ = 0.50, Rs = 10, and λ = 0.9. First: Da = 0.2 at $Ra_c^{(s)} = 20.6422$; Second Da = 0.1 at $Ra_c^{(s)} = 20.3396$ and the vertical direction at y = 20*

Figure 8 is a 3D Plots Showing the Behavoir of heavy Carbon-Rich Plumes (the yellow convection rolls) as permeability varies in the upper boundary of the anisotropic porous medium

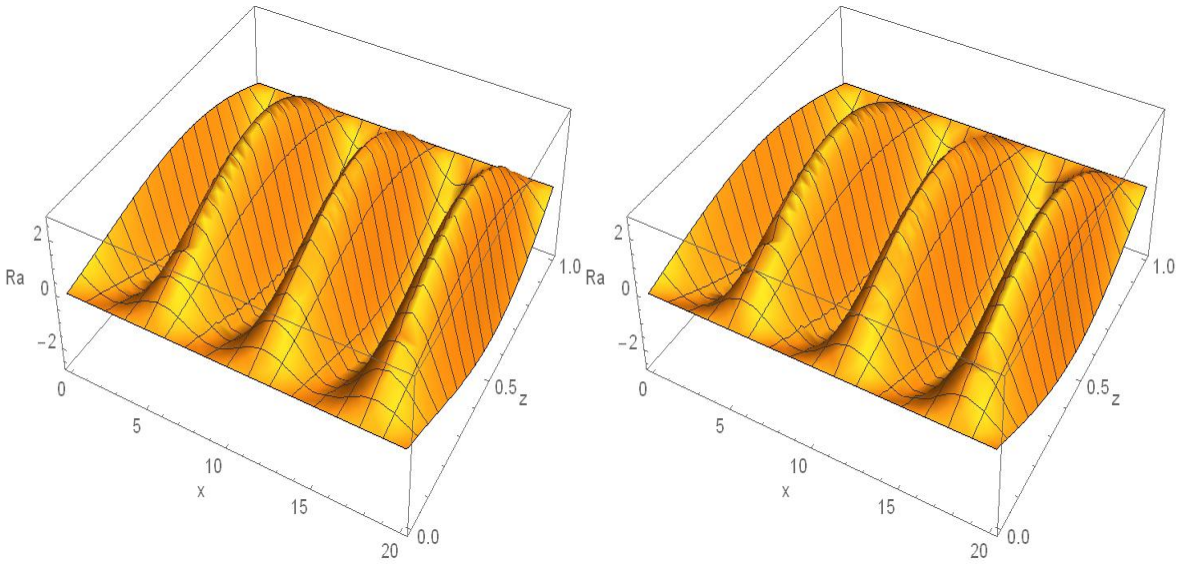

Figure 8: 3D plots showing the behavior of the heavy carbon-rich plume when permeability, λvaries and fixed values of $Da = 0.2,\ \xi = 0.50,\ Le = 1, Rs = 10,\ Ra_c^{(s)} = 20.6244$ *at* $\lambda = 0.9$ *and* $Ra_c^{(s)} = 28.2152$ *at* $\lambda = 0.1$ *were* $z = 0.5$

5. Conclusion

The onset of Rayleigh-Benard convection in CO_2 sequestration in the anisotropic porous medium as affected by temperature gradient and first-order chemical reaction is studied analytically using linear stability analysis. The linear theory provides the onset criteria for stationary convection in the anisotropic porous medium and the following conclusions are drawn;

1. When $Da < 0.2$, a conversion of about 10% is achieved. The term conversion is a ratio of how much reactant has reacted. While $Da > 10$, indicates a conversion of about 90% is expected. This means that as the Damköhler number increases, it is expected that the sequestered CO_2 must decrease. This in conjunction with the result obtained in Figure 2, which showed that for an increase in Da from $0.0001 - 0.5$, a decrease in the concentration level in the system was observed from $z = -1\ to\ 1$. This means that in the presence of chemical reaction the concentration level of the sequestered CO_2 decreases. Hence as Da increases, fully developed convection is characterized by vertical plumes emerging from the upper boundary surface layer.
2. An increase in the Damköhler number, rapidly decreases the concentration level of sequestered CO_2 in the system. This means that in the presence of perturbation where heating, chemical reaction and a change in density occurs, the concentration level of the sequestered CO_2 in turn decreases.
3. In the anisotropic porous medium, a gradual increase in the solute reaction rate to diffusion rate from $Da = 0.1$ to $Da = 0.2$, has a significant effect on the instability of the system from $\xi > 1$ to $\xi < 1$. At low permeability, the onset of instability in the stationary convection mode is still facilitated at $\xi < 1$, while there is a rapid delay in the onset of instability at $\xi > 1$. This thus means that (with respect to the onset of instability) varying the ratio of horizontal solute and thermal diffusivity to vertical solute and thermal diffusivity does have a significant effect at $\xi < 1$ than at $\xi > 1$ even in areas of lower permeability. At high permeability regions, the onset of instability in the stationary convection mode is very much facilitated at $\xi < 1$, while there is only a slight/minor delay in the onset of instability in the anisotropic porous medium at $\xi > 1$. This thus means that (with respect to the onset of instability) varying the ratio of horizontal solute and thermal diffusivity to vertical solute and thermal diffusivity does have a significant effect at $\xi < 1$ than at $\xi > 1$ in areas of high permeability. This means that for both permeability ranges, at $\xi < 1$ is a suitable medium for convective instability of CO_2 sequestration in the anisotropic porous medium.

Our results show that the linear stability theory accurately displays the final stage of stability and the onset of convective instability of CO_2 sequestration in a porous medium for the parameters explored. This thus means

that for changes in permeability of the porous medium at high reaction rate (when the solute reaction rate dominates the diffusion rate), there is a substantial effect on instability in the anisotropic porous medium ($\xi < 1$) Thus, it is recommended that in the Eastern Niger Delta region, the anisotropic porous medium (even as permeability changes) poses a more suitable medium for convective instability of sequestered CO_2 because the solute and thermal diffusivity vary and do not have the same value in different directions and hence a short-term amount of carbon dioxide dissolves rapidly

References

[1]. Metz, B.; Davidson, O.; Coninck, H.C.; Loos, M.; Meyer, L.A. IPCC Special Report on Carbon Dioxide Capture and Storage, prepared byWorking Group III of the Intergovernmental Panel on Climate Change. 2005.

[2]. Bachu, S.; Adams, J.J. Estimating CO_2 sequestration capacity in solution in deep saline aquifers. *Energy Conversion Management* 2003, 44, 3151-3175.

[3]. Spycher, N.; Pruess, K.; Ennis-King, J. CO_2-H_2O mixtures in the geological sequestration of CO_2: assessment and calculation of mutual solubilities from 12 ^oC to 100 ^oC and up to 600bar. *Geochim. Cosmochim. Acta.*2003, 67, 3015-3031.

[4]. Horton, C.W.; Rogers, F.T. Convection currents in a porous medium. *Journal of Applied Physics*1945, 16, 367-369.

[5]. Lapwood, E.R. Convection of a fluid in a porous medium. *Mathematical Proceedings of the Cambridge Philosophical Society* 1948, 44, 508-521.

[6]. Getling, A.V. Rayleigh-Benard convection. *Institute of Nuclear Physics Lomonosov Moscow State University* 2012, 7(7), 7702.

[7]. Caltagirone, J.P. Stability of a saturated porous layer subject to a sudden rise in surface temperature: Comparison between the linear and energy methods. *The Quarterly Journal of Mechanics and Applied Mathematics* 1980, 33, 47-58.

[8]. Ennis-King, J.; Preston, I.; Paterson, L. Onset of convection in anisotropic porous media subject to a rapid change in boundary conditions. *Physics of Fluids* 2005, 17, 084107.

[9]. Haddad, S. Thermal convection in a rotating anisotropic fluid saturated Darcy porous medium. *Physics of Fluids*2017, 2(3), 44.

[10]. Vadasz, P. Coriolis effect on gravity-driven convection in a rotating porous layer heated from below. *Journal of Fluid Mechanics*1998, 376, 351-375.

[11]. Xu, X.;Chen, S.; Zhang, Z. Convective stability analysis of the long-term storage of carbon dioxide in deep saline aquifers. *Advances in water resources* 2006, 29, 397-408.

[12]. Rapaka, S.; Chen, S.; Pawar, R.; Stauffer, P.H.; Zhang, D. Non-modal growth of perturbations in density-driven convection in porous media. *Journal of Fluid Mechanics* 2008, 609, 285-303.

[13]. Hassanzadeh, H.; Pooladi-Darvish, M.; Keith, D.W. Stability of a fluid in a horizontal saturated porous layer: Effect of non-linear concentration profile, initial and boundary conditions. *Transport Porous Medium* 2006, 65, 193-211.

[14]. Riaz, A.; Hesse, M.; Tchelepi, H.A.; Orr, F.M. Onset of convection in a gravitationally unstable diffusive boundary layer in porous media. *Journal of Fluid Mechanics* 2006, 548, 87-111.

[15]. Selim, A.; Rees, D.A.S. The stability of a developing thermal front in a porous medium: Nonlinear evolution. *Journal of Porous Media* 2007, 10(1), 17-34.

[16]. Wessel-Berg, D. On a linear stability problem related to underground CO_2 storage. *SIAM Journal on Applied Mathematics.*2009, 70(4), 1219-1238.

[17]. De Paoli, M.; Zonta, F.; Soldati, A. Influence of anisotropic permeability on convection in porous media: Implication for geological Carbon dioxide sequestration. *Physics of Fluids* 2016, 28, 056601.

[18]. Alex, S.M.; Patil, P.R. Thermal instability in an anisotropic rotating porous medium. *Journal of Heat and Mass Transfer* 2000, 36, 159-163.

[19]. Malashetty, M.S.; Swamy, M. The effect of rotation on the onset of convection in a horizontal anisotropic porous layer. *An International Journal of Thermal Sciences* 2007, 46, 1023-1032.

[20]. Vanishree, R.K.; Siddheshwar, P.G. Effect of rotation on thermal convection in an anisotropic porous medium with temperature-dependent viscosity. *Journal on Transport in Porous Media* 2010, 81, 73-87.
[21]. Kumar, A.; Bhadauria, B.S. Thermal instability in a rotating anisotropic porous layer saturated by a viscoelastic fluid. *An International Journal of Nonlinear Mechanics* 2011, 46, 47-56.
[22]. Malashetty, M.S.; Biradar, B.S. The onset of double diffusive reaction-convection in an anisotropic porous layer. *Physics of Fluids* 2011, 23, 064102.
[23]. Ghesmat, K.; Hassanzadeh, H.; Abedi, J. The impact of geochemistry on convective mixing in a gravitationally unstable diffusive boundary layer in porous media: CO_2 storage in saline aquifers. *A Journal of Fluid Mechanics* 2011, 673, 480-512.
[24]. Andres, J.T.H.; Cardoso, S.S. Onset of convection in a porous medium in the presence of chemical reaction. *Physical Review E*2011, 83, 046312.
[25]. Andres, J.T.H.; Cardoso, S.S. Convection and reaction in a diffusive boundary layer in a porous medium: Nonlinear dynamics. *An Interdisciplinary Journal of Nonlinear Science.* 2012, 22, 037113.
[26]. Ward, T.A.; Cliffe, K.A.; Jensen, O.E.; Power, H. Dissolution driven porous medium convection in the presence of chemical reaction. *Journal of Fluid Mechanics* 2014, 747, 316-349.
[27]. Fanchi, J.R. Principles of Applied Reservoir Simulation (4^{th} Ed). Texas Christian University, Fort Worth, Texas 2018.
[28]. Hill, A.A.; Morad, M.R. Convective stability of Carbon sequestration in anisotropic porous media. *Proceedings of the Royal Society a Mathematical, Physical and Engineering Sciences* 2014, 470, 20140373.
[29]. Vo, L.; Hadji, L. Weakly nonlinear convection induced by the sequestration of CO_2 in a perfectly impervious geological formation. *Physics of Fluids* 2017, 29, 127101.
[30]. Wanstall, T. C.; Hadji, L. A step function density profile model for the convective stability of CO_2 geological sequestration. *Journal of Environmental Mathematics* 2018, 1-26.